Materials Transactions, Vol. 50, No. 8 (2009) pp. 1978 to 1984

A Thermochemical Database for the Solar Cell Silicon Materials

Kai Tang[1], Eivind J. Øvrelid[1], Gabriella Tranell[2] and Merete Tangstad[2]

[1]*SINTEF Materials and Chemistry, N-7465 Trondheim, Norway*
[2]*Norwegian University of Science and Technology, N-7491 Trondheim, Norway*

The fabrication of solar cell grade silicon (SOG-Si) feedstock involves processes that require direct contact between solid and liquid phases at near equilibrium conditions. Knowledge of the phase diagram and thermochemical properties of the Si-based system is therefore important for providing boundary conditions in the analysis of processes. A self-consistent thermodynamic description of the Si-Ag-Al-As-Au-B-Bi-C-Ca-Co-Cr-Cu-Fe-Ga-Ge-In-Li-Mg-Mn-Mo-N-Na-Ni-O-P-Pb-S-Sb-Sn-Te-Ti-V-W-Zn-Zr system has recently been developed by SINTEF Materials and Chemistry. The assessed database has been designed for use within the composition space associated with SoG-Si materials. The thermochemical database has further been extended to calculate the surface tensions of liquid Si-based melts. In addition to thermochemical and phase equilibrium calculation, several surface-related properties (temperature and composition gradients, surface excess quantity etc.) are able to simulate simultaneously using the database. The databases can be regarded as the state-of-art equilibrium relations in the Si-based multicomponent system. [doi:10.2320/matertrans.M2009110]

(Received March 30, 2009; Accepted May 18, 2009; Published July 1, 2009)

Keywords: *thermochemical database, solar cell grade silicon, surface properties*

1. Introduction

The success of producing and refining Si feedstock materials to ultra high purity depends heavily on the availability and reliability of thermodynamic, kinetic and other physical data for the most common and important SoG-Si trace elements. For example, knowledge of the phase diagram and thermochemical properties of the Si-based system is important for providing boundary conditions in the analysis of processes. However, thermodynamic and kinetic data for these elements in the ppm and ppb ranges are scarce and often unreliable. More importantly, to our knowledge, no dedicated SoG-Si database exists which has gathered and optimized existing data on high purity Si alloys.

Aluminum, boron, carbon, iron, nitrogen, oxygen, phosphorus, sulfur and titanium are the common impurities appearing in the SoG-Si feedstock. Arsenic and antimony are frequently used as doping agents. Transition metals (Co, Cu, Cr, Fe, Mn, Mo, Ni, V, W, Zr), alkali and alkali-earth impurities (Li, Mg, Na) as well as Bi, Ga, Ge, In, Pb, Sn, Te and Zn may appear in the SoG-Si feedstock. The composition space of these impurities generally ranges from ppb to a few percent, as illustrated in Fig. 1.

In this paper, a self-consistent thermodynamic description of the Si-Ag-Al-As-Au-B-Bi-C-Ca-Co-Cr-Cu-Fe-Ga-Ge-In-Li-Mg-Mn-Mo-N-Na-Ni-O-P-Pb-S-Sb-Sn-Te-Ti-V-W-Zn-Zr system is introduced. The database covers all 34 silicon-impurity binary systems. Among these binary silicon-containing systems, the Si-Al, Si-As, Si-B, Si-C, Si-Fe, Si-N, Si-O, Si-P, Si-S, Si-Sb and Si-Te systems have been thermodynamically "re-optimized" based primarily on the assessed experimental information. Since thermodynamic calculations for the impurities in SoG-Si feedstock are normally multi-dimensional in nature, Gibbs energies of 36 other binary systems have also been included in the database. In this way, the effect of other impurities on the phase equilibria of principle impurity in SoG-Si materials can be reliably evaluated. Systematic validation of the database has been carried out using the experimental data for Si-based multi-component systems, and examples of the validation are given in the following section.

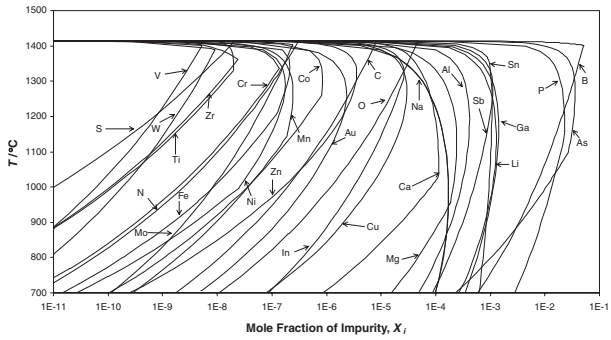

Fig. 1 The composition space associated with the SoG-Si feedstock.

The Czochralski method of growing single crystal silicon is affected by thermo-capillary convection. Temperature and concentration gradients at the free surface of the melt give rise to surface tension-driven Marangoni flow, which can lead to crystal defects, if it is sufficiently large. To this end, the assessed thermochemical database has further been extended to calculate the surface tensions of liquid Si-based melts, subject to the constraint of Gibbs energy minimization. In addition to thermodynamic properties, the temperature and composition gradients of surface tension in Si-based melts can be simultaneously calculated using the database. The databases can be regarded as the state-of-art equilibrium relations in the Si-based multicomponent system.

2. Thermodynamic Description

2.1 Element and stoichiometric compound

The SGTE formulism[1)] has been selected for the representation of the Gibbs energy of the pure elements and the stoichiometric compounds. Compounds with a narrow range of homogeneity, for example SiB_6 and SiB_3, are treated as stoichiometric compounds in the database.

2.2 Solution

The liquid Si-based solution, here abbreviated as l, is described using a simple polynomial expression based on a substitutional solution with random mixing. The same model is employed for the diamond-structured Si-rich solid phase, denoted as s. The Gibbs energies of the liquid and solid Si-based phases are given by the following equation:

$$G_m^\phi = x_{\mathrm{Si}}^\phi {}^0G_{\mathrm{Si}}^\phi + \sum_{i\neq \mathrm{Si}} x_i^\phi {}^0G_i^\phi + RT\left(x_{\mathrm{Si}}^\phi \ln x_{\mathrm{Si}}^\phi + \sum_{i\neq \mathrm{Si}} x_i^\phi \ln x_i^\phi\right) + {}^{\mathrm{Ex}}G_m^\phi \quad (\phi = l, s) \tag{1}$$

where ${}^0G_{\mathrm{Si}}^\phi$ and ${}^0G_i^\phi$ are, respectively, the molar Gibbs energy of Si and element i with the phase ϕ in a nonmagnetic state, The second term is the contribution of ideal mixing. The excess Gibbs energy, ${}^{\mathrm{Ex}}G_m^\phi$, is expressed in the Redlich-Kister polynomial:

$${}^{\mathrm{Ex}}G_m^\phi = \sum_i \sum_j x_i^\phi x_j^\phi \sum_{k=0}^{n} {}^kL_{ij}^\phi (x_i^\phi - x_j^\phi)^k \tag{2}$$

Since the concentrations of impurities in solar cell grade silicon are in the range from ppb to a few percent, it is not necessary to take ternary interaction parameters into account.

The activity coefficient of impurity, i, in a multicomponent system is given by eq. (3):

$$RT\ln\gamma_i^\phi = {}^{\mathrm{Ex}}G_m^\phi + \frac{\partial {}^{\mathrm{Ex}}G_m^\phi}{\partial x_i^\phi} - \sum_{j=1}^{n} x_j^\phi \frac{\partial {}^{\mathrm{Ex}}G_m^\phi}{\partial x_j^\phi} \tag{3}$$

For SoG-Si materials, $x_i^\phi \to 0$ and $x_{\mathrm{Si}}^\phi \to 1$, so the Henrian activity coefficient of component i can be approximately expressed:

$$\gamma_i^\phi \approx \exp\left(\sum_{k=0}^{n} {}^kL_{\mathrm{Si}-i}^\phi \Big/ RT\right) \quad (\phi = l, s) \tag{4}$$

The assessed model parameters, ${}^kL_{ij}^\phi$, for the liquid and solid phases in the Si-rich Si-Al-B-C-Fe-P system are listed in Table 1. Thermodynamic descriptions of the solid compounds are taken from the SGTE pure substance thermochemical database.

2.3 Equilibrium distribution coefficient

Segregation effects at the liquid-solid interface are controlled by the equilibrium distribution coefficient, k_i^{eq}, which is defined as the ratio of the solidus and the liquidus concentrations in atomic fractions:

$$k_i^{\mathrm{eq}} = x_i^{\mathrm{s}}/x_i^{\mathrm{l}} \tag{5}$$

Since the distribution coefficient controls the incorporation of impurities in the crystal during crystal growth and zone refining, it is one of the most important parameters that can be directly obtained from the thermochemical database. It is worth noting that the distribution coefficient determined by the ratio of volume concentrations, in cm^{-3}, can be related to the distribution coefficient by introducing the density ratio of liquid and solid silicon:

$${}^Vk_i^{\mathrm{eq}} = (\rho_{\mathrm{Si}}^{\mathrm{liq.}}/\rho_{\mathrm{Si}}^{\mathrm{sol.}})k_i^{\mathrm{eq}} \approx 1.1k_i^{\mathrm{eq}} \tag{6}$$

Applying the phase equilibrium rule to this case results in the formula for the determination of equilibrium distribution coefficient:

Table 1 Thermodynamic descriptions of the liquid and solid Si-rich Si-Al-B-C-Fe-P system in SI unit.

Liquid phase (J/mol)	Solid phase (J/mol)
${}^0L_{\mathrm{SiAl}}^{\mathrm{Liq}} = -11340 - 1.234T$	${}^0L_{\mathrm{SiAl}}^{\mathrm{Sol}} = 91800 - 14.51T$
${}^1L_{\mathrm{SiAl}}^{\mathrm{Liq}} = -3531 + 1.36T$	${}^0L_{\mathrm{SiB}}^{\mathrm{Sol}} = 66884 - 17.25T$
${}^2L_{\mathrm{SiAl}}^{\mathrm{Liq}} = 2265.4$	${}^0L_{\mathrm{SiC}}^{\mathrm{Sol}} = 90000 + 4.5T$
${}^0L_{\mathrm{SiB}}^{\mathrm{Liq}} = 17632 - 1.7632T$	${}^0L_{\mathrm{SiFe}}^{\mathrm{Sol}} = 137650 - 8.12T$
${}^1L_{\mathrm{SiB}}^{\mathrm{Liq}} = -3527 + 0.353T$	${}^0L_{\mathrm{SiP}}^{\mathrm{Sol}} = -21508 + 24.97T$
${}^0L_{\mathrm{SiC}}^{\mathrm{Liq}} = -15700 + 6.52T$	
${}^0L_{\mathrm{SiFe}}^{\mathrm{Liq}} = -164434.6 + 41.9773T$	
${}^1L_{\mathrm{SiFe}}^{\mathrm{Liq}} = 0 - 21.523T$	
${}^2L_{\mathrm{SiFe}}^{\mathrm{Liq}} = -18821.5 + 22.07T$	
${}^3L_{\mathrm{SiFe}}^{\mathrm{Liq}} = -9695.8$	
${}^0L_{\mathrm{SiP}}^{\mathrm{Liq}} = -141000 + 43.6T$	

$$k_i^{\mathrm{eq}} = \frac{\gamma_i^{\mathrm{l}}}{\gamma_i^{\mathrm{s}}} \exp\left(\frac{-\Delta^0 G_i^{\mathrm{fus}}}{RT}\right) \tag{7}$$

here $\Delta^0 G_i^{\mathrm{fus}}$ refers the Gibbs energy of fusion of impurity i at temperature T. Activity coefficients of impurity i in liquid and solid phases can be determined using eq. (4).

2.4 Retrograde solubility

Retrograde solubility describes the change in impurity concentration in a solid above the eutectic temperature, i.e. a maximum solubility is observed at a temperature $T_{\max}$ lower than melting temperature of silicon T_{m}, but above the eutectic temperature. In this frequently encountered case, impurities tend to precipitate upon cooling.

Weber[2] proposed a formula to determine the maximum retrograde temperature assuming the impurity behaves ideally in liquid solution and regularly in solid phase:

$$T_{\max} = \frac{\Delta H_{\mathrm{Si}}^m}{\Delta S_{\mathrm{Si}}^m - k_i^{\mathrm{eq}}[\ln(\Delta H_i^m) - \ln(\Delta H_i^m + \Delta H_{\mathrm{Si}}^m)]} \tag{8}$$

where ΔH_{Si}^m and ΔS_{Si}^m are the enthalpy and entropy changes for the fusion of pure silicon. Thermodynamically, retrograde solubility requires a large positive value for ΔH_i^m, the solid solution enthalpy of mixing.

Retrograde solubility can be usefully applied in solidification refining of impurities in SoG-Si materials. Yoshikawa and Morita proposed the methods for the removal of boron[3,4] and phosphorus[5] by addition of Al and Ti. Shimpo *et al.*[6] and Inoue *et al.*[7] reported the Ca addition method to remove boron and phosphorus in silicon. Application of the present thermochemical database in searching the candidate solidification refining alloy systems will be given in the following text.

2.5 Surface tension

Following the theoretical treatment given by Guggenheim[8] and Bulter,[9] a monolayer surface phase is assumed in equilibrium with the bulk liquid phase. Since the surface tension is the reversible work required to extend a surface by a unit area at constant temperature, pressure and composition, it is necessary to take the area into consideration for the Gibbs energies of the species in the surface phase. A fictitious species, "Area", is thus introduced to the surface phase.[10] The components of surface phase are

assumed to be "Area"-related: SiA_m, AlA_n, BA_p, OA_q, ...*etc.* The stoichiometric coefficients of the "Area"-related components can be determined by the normalized molar surface area of pure element:

$$m = A_i/A_0, \quad n = A_j/A_0, \quad \cdots \tag{9}$$

where $A_i, A_j, \cdots$ are the molar surface areas of pure elements and A_0 the normalization constant. The numerical value of A_0 is in principle arbitrary. For the best numerical performance of Gibbs energy minimization and for the sake of the common interfacial tension unit (mN/m), a value 1000 is used for A_0 in the present study.

The chemical potentials of components in the surface phase are determined by following equation:

$$\mu_i^S = \mu_i^0 + RT \ln a_i^S + A_i\sigma_i \tag{10}$$

here σ_i is the surface tension of pure element i and μ_i^0 the chemical potential of i in the bulk phase.

Elements B, C, O and N are normally either in the form of solid or gas in the temperature range of interest. The molar surface areas and surface tensions of the metastable B, C, O and N liquids have been estimated from the experimental values. The criterion of equilibrium between the bulk and surface phase leads to following equation for component i:

$$A_i(\sigma - \sigma_i) = RT(\ln a_i^S - \ln a_i^B) \tag{11}$$

Equation (11) can be used for the determination of the molar surface area of i, if the measured interfacial tension, σ, is available. A special code has been developed for this purpose.

At equilibrium, the following simple linear relation holds:[11)]

$$G = \sum_l b_l\mu_l \tag{12}$$

here b_l is the total molar amount of system component l in the system. This means that the chemical potential of the fictitious component, μ_{Area}, is equivalent to the surface tension of liquid melt, σ, in the unit of mN/m (because the normalization constant, A_0, is used with the unit m^2/mol). In this way, surface tension of a multicomponent melt can be directly determined by Gibbs energy minimization technique under the following mass and an additional "Area" balance constraints:

$$\sum_i \sum_l (a_{il}^B n_i^B + a_{il}^S n_i^S) = b_l \tag{13}$$

$$\sum_l (A_l^S/A_0) n_l^S = A/A_0 \tag{14}$$

where a_{il}^B and a_{il}^S are the coefficients of the stoichiometric matrices of components in bulk and surface phases, n_i^B and n_i^S are the molar numbers of species in bulk and surface phases, respectively.

3. Typical Examples

Thermochemical assessments for the Si-Al, Si-B, Si-C, Si-Fe and Si-P binary systems will briefly be introduced in this section. Typical examples of the database calculation results are presented as diagrams.

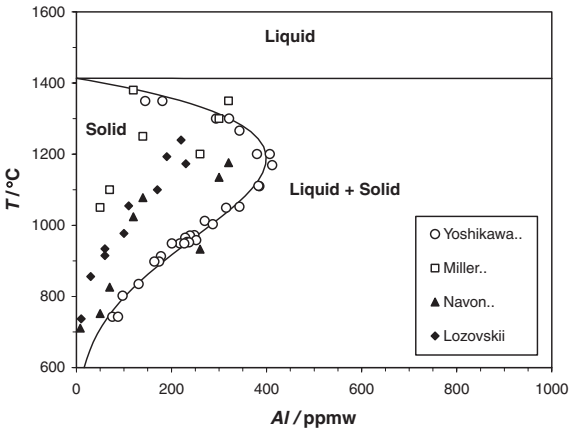

Fig. 2 The assessed Si-Al system in the Si-rich domain.

3.1 The Si-Al system

The reassessment of the Si-Al binary system has been carried out based mainly on the experimental solubility data reported by Yoshikawa and Morita.[12)] The measured solubilities given by Miller and Savage,[13)] Navon and Chernyshov,[14)] Lozovskii and Udyanskaya[15)] are also shown in the diagram for comparison. Activities of Al in liquid Si measured by Miki *et al.*[16,17)] and Ottem[18)] were also taken into account in the assessment of the liquid phase. Figure 2 shows the calculated phase equilibria in the Si-rich region of the Si-Al system.

3.2 The Si-B system

Reassessment of the Si-B system was based primarily on the model parameters given by Fries and Lukas.[19)] Modifications have been made to the thermodynamic properties of the liquid and solid Si-based mixture phases: experimental liquidus data reported by Brosset,[20)] Armas *et al.*,[21)] Male and Salanoubat,[22)] solid solubility data reported by Trumbore,[23)] Hesse,[24)] Samsonov and Sleptsov[25)] and Taishi *et al.*,[33)] as well as boron activities in the liquid phase measured by Inoue *et al.*[7)] Zaitsev *et al.*,[26)] Yoshikawa and Morita[27)] and Noguchi *et al.*[28)] were all used to determine the model parameters. Figure 3 shows the new assessed phase equilibria in the Si-rich Si-B system. The equilibrium distribution coefficient calculated from the present assessment is 0.757, which is close to the recent experimental value,[29)] 0.751.

3.3 The Si-C system

The new assessment for the Si-C system was based primarily on experimental SiC solubility data in liquid silicon given by Ottem,[18)] Scace and Slack,[30)] Hall,[31)] Iguchi,[32)] Kleykamp and Schumacher,[33)] Oden and McCune.[34)] Solid solubility data given by Nozaki *et al.*,[35)] Bean[36)] and Newman[37)] were used to determine the properties of solid solution. The eutectic composition reported by Nozaki *et al.*[35)] and Hall[31)] and peritectic transformation temperature determined by Scace[30)] and Kleykamp[33)] were also used in the thermodynamic optimization. Thermodynamic description of the SiC compound was taken from an early assessment.[38)] The calculated SiC solubilities in liquid and solid Si-C solutions are compared with the experimental values in Fig. 4. Calculated SiC solubilities in

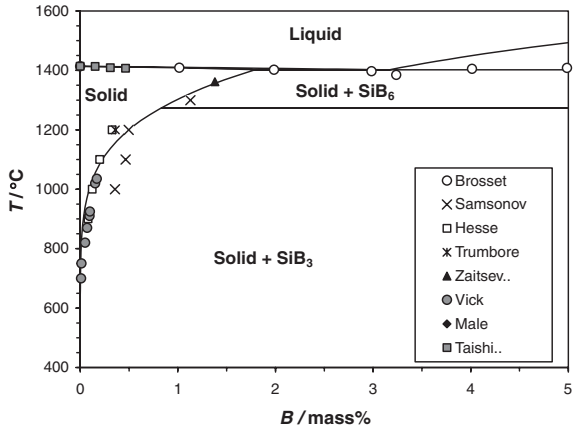

Fig. 3 The assessed Si-B system in the Si-rich domain.

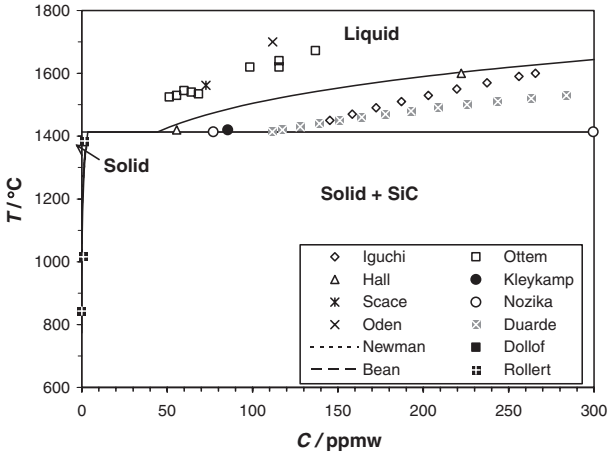

Fig. 4 The assessed Si-C system in the Si-rich.

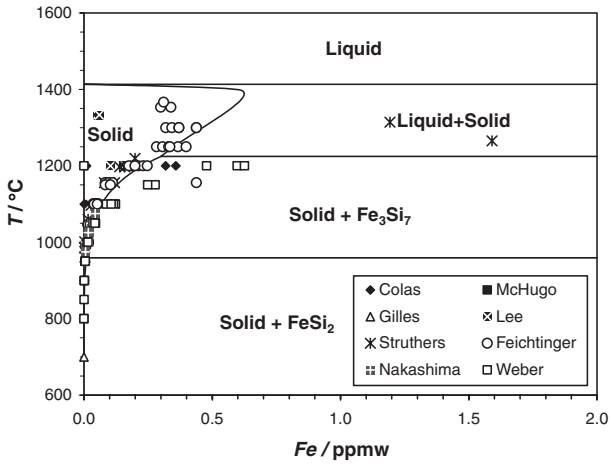

Fig. 5 The assessed Si-Fe system in the Si-rich domain.

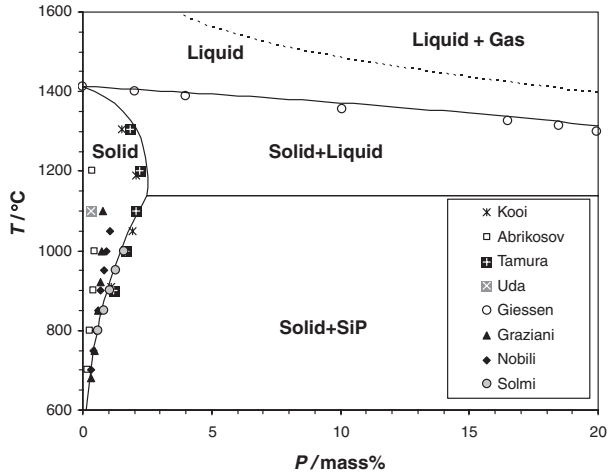

Fig. 6 The assessed Si-P system in the Si-rich domain.

liquid silicon have been confirmed by the most recent measurements carried out by Dakaler and Tangstad.[39]

3.4 The Si-Fe system

Experimental information on the solubility of Fe in solid silicon was reviewed by Istratov *et al.*[40] The retrograde solubility of iron above the eutectic temperature was reported by Trumbore,[23] Feichtinger[41] and Lee *et al.*[42] The solubility of iron below the eutectic temperature was studied by Lee *et al.*,[42] Mchugo *et al.*,[43] Colas and Weber,[44] Weber,[45] Struthers,[46] Nakashima *et al.*[47] and Gills *et al.*[48] Thermodynamic description of the solid diamond phase was optimized using the above experimental phase equilibrium information. Parameters for the excess Gibbs energy of the liquid Si-Fe phase were optimized by Lacaze and Sundman,[49] based primarily on the assessment by Chart.[50] The measured thermodynamic properties of Fe in molten Si given by Miki *et al.*[51] and Hsu *et al.*[52] are reproducible using the assessed model parameters. Figure 5 shows the new assessed phase equilibria in the Si-rich Si-Fe system in the temperature range of interest.

3.5 The Si-P system

Solubility of phosphorus in liquid and solid silicon were reported by Zaitsev *et al.*,[53] Carlsson *et al.*,[54] Giessen and Vogel,[55] Korb and Hein,[56] Miki *et al.*,[57] Anusionwu *et al.*,[58] Ugai *et al.*[59] Uda and Kamoshida,[60] Kooi,[61] Abrikosov *et al.*,[62] Solmi *et al.*,[63] Nobili *et al.*[64] and Tamura.[65] The Figure 6 is the partial Si-P phase diagram calculated using the present database.

4. Application of the Thermochemical Database

4.1 Solubility and distribution coefficient

The assessed thermodynamic properties of liquid and solid Si-based solutions can be used to evaluate the influence of third element on the solubility of the main impurity in silicon melts. For example, the effects of other impurity elements on the solubilities of C in pure Si melt can be evaluated by the following equation:

$$\ln x_{\mathrm{C}}^{\mathrm{liq}} \cong -\ln K_{\mathrm{SiC}}^{0} - \ln \gamma_{\mathrm{C}}^{\mathrm{Si\text{-}C}} + x_i(\ln \gamma_i^{\mathrm{Si}\text{-}i} - \ln \gamma_{\mathrm{C}}^{\mathrm{Si}\text{-}i} - \ln \gamma_{\mathrm{C}}^{i\text{-}\mathrm{C}}) \qquad (15)$$

where K_{SiC}^{0} is the equilibrium constant for the reaction: $\underline{\mathrm{Si}} + \underline{\mathrm{C}} = \mathrm{SiC}_{\beta}$. $\gamma_{\mathrm{C}}^{\mathrm{Si\text{-}C}}$ and $\gamma_{\mathrm{C}}^{i\text{-}\mathrm{C}}$ are the activity coefficient of carbon in Si-C and i-C binary melts, respectively. $\gamma_i^{\mathrm{Si}\text{-}i}$ is the liquid activity coefficients of i in Si-i binary melt. Figure 7 shows the model calculation results. Additions of Zr, P, B, Zn, As, Mn and Al to liquid silicon increase carbon solubility whereas additions of O, Cr, Cu, Ca, Fe, Ni, S and N have the

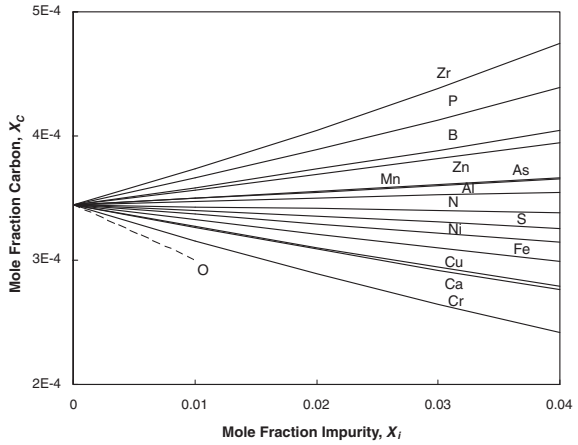

Fig. 7 Effect of element on the carbon solubility in liquid silicon.

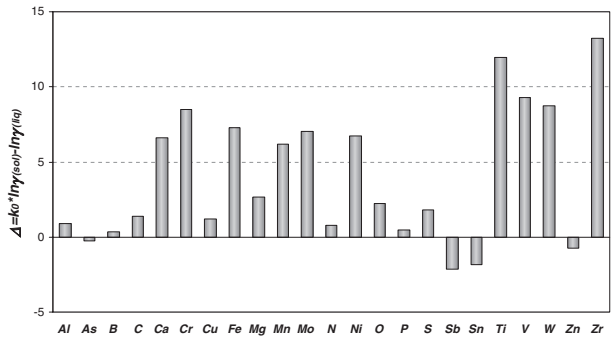

Fig. 8 The effect of third element on the equilibrium distribution coefficient of the primary impurity.

opposite effect. The model calculations agree with the experimental results reported by Yanaba *et al.*[66]

Since the impurities in SoG-Si feedstock are normally multi-dimensional in nature, it is important to estimate the influence of the other impurities on the equilibrium distribution coefficient of the main impurity in liquid Si. A simple relation has been derived using the Henrian activity coefficients:

$$\ln {}^3k_i^{eq} \cong \ln {}^2k_i^{eq} + x_j^l({}^2k_j^{eq} \ln \gamma_{Si\text{-}j}^s - \ln \gamma_{Si\text{-}j}^l) = \ln {}^2k_i^{eq} + x_j^l \Delta \quad (16)$$

here ${}^2k_i^{eq}$ and ${}^3k_i^{eq}$ are, respectively, the distribution coefficient of i in Si-i binary and Si-i-j ternary systems. Calculated Δ values for different impurities in pure Si are shown in Fig. 8. Most of the common impurities in pure Si have a positive contribution to the equilibrium distribution coefficient, *i.e.* the appearance of secondary impurities will increase the distribution coefficient of the primary impurity in pure silicon, except As, Sb, Sn and Zn.

Solvent refining is a purification process in which recrystallization takes place from the supersaturated melt depending on the segregation behavior of different elements. The assessed thermochemical database can be used to evaluate the possible candidates for the solvent refining of B in Si. Figure 9 shows the calculated B segregation coefficients in Si-Al melts which are closed to the experimental values.[3,4] The model also predicts that the removal of B by Si-Zn melt is even more efficient than the Si-Al melt.

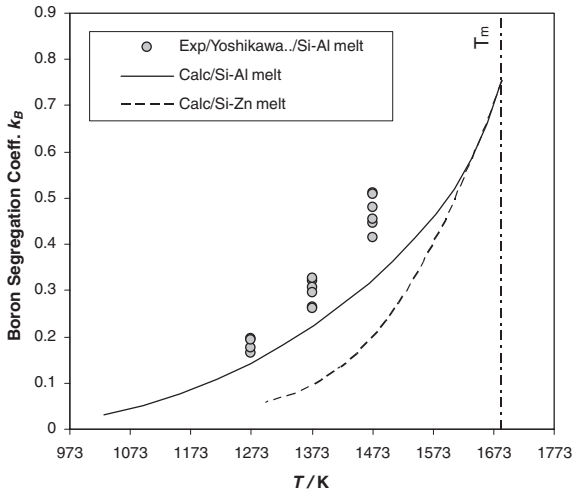

Fig. 9 Boron segregation coefficients in the solidification refining of Si-Al and Si-Zn melts.

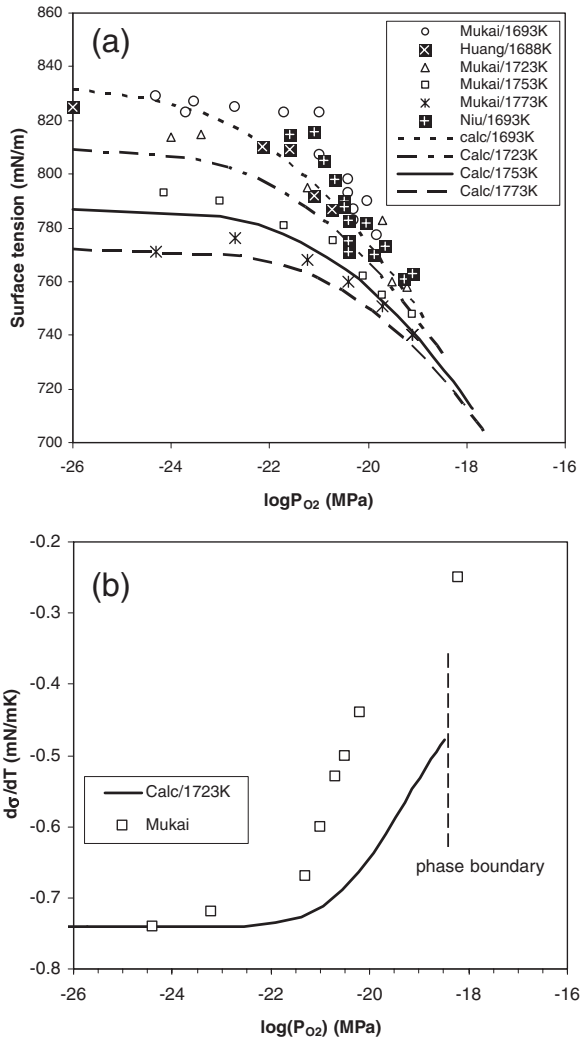

Fig. 10 Calculated (a) surface tension of Si-O melt and (b) its temperature gradient.

4.2 Surface tension

The modeled surface tension and its temperature gradient for the Si-O melts at different oxygen partial pressures are shown in Fig. 10. Thermodynamic descriptions of the bulk

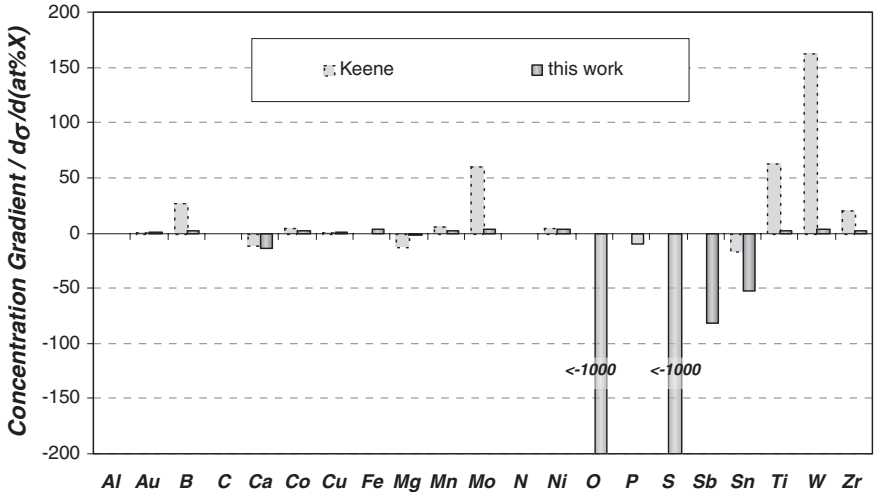

Fig. 11 Calculated concentration gradients of impurities in silicon melt.

Table 2 Thermodynamic descriptions of the surface and bulk phases in Si-O system in SI unit.

Bulk phase: (Si, O) mixture	Surface phase: ($SiA_{45.8}$-OA_{232}) mixture
μ^0_{Si} from Ref. 1)	$\mu^S_{Si} = \mu^0_{Si} + 58257 - 11.46T$
μ^0_O from Ref. 1)	$\mu^S_O = \mu^0_O + 2000 - 0.2T$
${}^0L^{Liq}_{SiO} = -303630 + 50T$	${}^0L^{Liq}_{SiA_{45.8}\text{-}OA_{232.2}} = -273267 + 45T$

and surface phases in the Si-O system are given in Table 2. The calculation results can reproduce the experimental data[67–71] within their uncertainties.

Using the surface tension implemented Si-based thermochemical database, the surface-related properties (*e.g.* temperature and composition gradients, surface excess quantity, etc.) are readily obtained. Figure 11 shows the calculated composition gradients of impurities in silicon melt. The composition gradient values estimated by Keene[72] are also given in the diagram for comparison. In addition to the surface tension, phase equilibria and thermochemical properties of the corresponding system can simultaneously be obtained in the calculation. This may provide more efficient and accurate ways to simulate practical problems.

5. Conclusions

A self-consistent thermodynamic description of the Si-Ag-Al-As-Au-B-Bi-C-Ca-Co-Cr-Cu-Fe-Ga-Ge-In-Li-Mg-Mn-Mo-N-Na-Ni-O-P-Pb-S-Sb-Sn-Te-Ti-V-W-Zn-Zr system has recently been developed by SINTEF Materials and Chemistry. The assessed database has been designed for use within the composition space associated with the SoG-Si feedstock. Among the 33 binary silicon-containing systems, the Si-Al, Si-As, Si-B, Si-C, Si-Fe, Si-N, Si-O, Si-P, Si-S, Si-Sb and Si-Te systems have been thermodynamically "re-optimized" based primarily on the assessed experimental information. The thermochemical database has also been further extended to simulate the surface tension of liquid Si-based melts.

The calculated phase equilibria in the Si-rich Si-Al, Si-B, Si-C, Si-Fe and Si-P systems have been illustrated in the present paper. Typical examples for the application of the present database to evaluate the effect of second impurities on the solubility and distribution coefficient of primary impurity in liquid silicon were also discussed. The calculated surface tension and its temperature coefficient in liquid Si-O melts are in good agreement with the experimental values. The surface tension temperature and composition coefficients for the common impurities have finally been evaluated.

Acknowledgments

Financial support from the Norwegian Research Council is gratefully acknowledged.

REFERENCES

1) T. Dinsdale: Calphad **15** (1991) 317–425.
2) E. R. Weber: Appl. Phys. A **30** (1983) 1–22.
3) T. Yoshikawa, K. Arimura and K. Morita: Metall. Mat. Trans. B **36** (2005) 837–842.
4) T. Yoshikawa and K. Morita: Metall. Mat. Trans. B **36** (2005) 731–736.
5) T. Yoshikawa and K. Morita: Sci. Tech. Adv. Mat. **4** (2003) 531–537.
6) T. Shimpo, T. Yoshikawa and K. Morita: Metall. Mat. Trans. B **35** (2004) 277.
7) G. Inoue, T. Yoshikawa and K. Morita: High Temp. Mat. Proce. **22** (2003) 221–226.
8) E. A. Guggenheim: Trans. Faraday Soc. **41** (1945) 150–156.
9) J. A. V. Bulter: Proce. Royal Soc. A **135** (1932) 348–375.
10) P. Koukkari and R. Pajarre: Calphad **30** (2006) 18–26.
11) G. Eriksson and K. Hack: Metall. Trans. B **21** (1990) 1013–1023.
12) T. Yoshikawa and K. Morita: J. Electrochem. Soc. **150** (2003) G465–G468.
13) R. C. Miller and A. Savage: J. Appl. Phys. **27** (1956) 1430–1432.
14) D. Navon and V. Chernyshov: J. Appl. Phys. **28** (1957) 823–824.
15) V. N. Lozovskii and A. I. Udyanskaya: Izv. Akad. Nauk SSSR, Neorg. Mater. **4** (1968) 1174–1175.
16) T. Miki, K. Morita and N. Sano: Mater. Trans. JIM **40** (1999) 1108–1116.
17) T. Miki, K. Morita and N. Sano: Metall. Mat. Trans. B **29** (1998) 1043–1049.
18) L. Ottem: SINTEF Report STF34 F93027, 1993, Trondheim, Norway.
19) S. Fries and H. L. Lukas: COST507 (1998) 77.
20) C. Brosset and B. Magnusson: Nature **187** (1960) 54–55.
21) B. Armas, G. Male, D. Salanoubat, C. Chatillon and M. Allibert: J. Less Com. Met. **82** (1981) 245–254.
22) G. Male and D. Salanoubat: Rev. Inter. Hau. Temp. Ref. **18** (1981)

109–120.
23) F. A. Trumbore: Bell Sys. Tech. J. **39** (1960) 205–233.
24) J. Hesse: Z. Metallkd. **59** (1968) 499–502.
25) G. V. Semenova, T. P. Sushkova, E. A. Dolgopolova and A. A. Morozova: Rus. J. Inorg. Chem. **48** (2003) 582–584.
26) I. Zaitsev and A. A. Kodentsov: J. Phase Equ. **22** (2001) 126–135.
27) T. Yoshikawa and K. Morita: Mater. Trans. **46** (2005) 1335–1340.
28) R. Noguchi, K. Suzuki, F. Tsukihashi and N. Sano: Metall. Mat. Trans. B **25** (1994) 903–907.
29) B. C. Sim, K. H. Kim and H. W. Lee: J. Cryst. Growth **290** (2006) 665–669.
30) R. I. Scace and G. A. Slack: J. Chem. Phys. **30** (1959) 1551–1555.
31) R. N. Hall: J. Appl. Phys. **29** (1958) 914–917.
32) Y. Iguchi and T. Narushima: 1st Int. Conf. on Proce. Mat. for Proper. Ed. by H. Henein and T. Oki, (The Minerals. Metals & Matenals Soc., 1993) pp. 437–439.
33) H. Kleykamp and G. Schumacher: Ber. Bun. Phys. Chem. **97** (1993) 799–805.
34) L. L. Oden and R. A. Mccune: Metall. Trans. A **18** (1987) 2005–2014.
35) T. Nozaki, Y. Yatsurugi and N. Akiyama: J. Electrochem. Soc. **117** (1970) 1566–1568.
36) R. Bean and R. C. Newman: J. Phys. Chem. Solids **32** (1971) 1211–1219.
37) R. C. Newman: Mat. Sci. Eng. B **36** (1996) 1–12.
38) J. Grobner, H. L. Lukas and J. C. Anglezio: Calphad **20** (1996) 247–254.
39) H. Dalaker and M. Tangstad: 23rd Euro. Photo. Sol. Energy Conf., (Valencia, Spain, 2008).
40) A. A. Istratov, H. Hieslmair and E. R. Weber: Appl. Phys. A **69** (1999) 13–44.
41) H. Feichtinger: Acta Physica Austriaca **51** (1979) 161–189.
42) Y. H. Lee, R. L. Kleinhenz and J. W. Corbett: Appl. Phys. Lett. **31** (1977) 142–144.
43) S. A. Mchugo, R. J. McDonald, A. R. Smith, D. L. Hurley and E. R. Weber: Appl. Phys. Lett. **73** (1998) 1424–1426.
44) G. Colas and E. R. Weber: Appl. Phys. Lett. **48** (1986) 1371–1373.
45) Weber and H. G. Riotte: J. Appl. Phys. **51** (1980) 1484–1488.
46) J. D. Struthers: J. Appl. Phys. **27** (1956) 1560–1560.
47) H. Nakashima, H. Nakashima and K. Hashimoto: Jpn. J. Appl. Phys. **27** (1988) 1542–1543.
48) D. Gilles, W. Schröter and W. Bergholz: Phys. Rev. B **41** (1990) 5770.
49) J. Lacaze and B. Sundman: Metall. Trans. A **22** (1991) 2211–2223.
50) T. G. Chart: High Temp. High Pres. **2** (1970) 461–470.
51) T. Miki, K. Morita and N. Sano: Metall. Mat. Trans. B **28** (1997) 861–867.
52) C. C. Hsu, A. Y. Polyakov and A. M. Samarin: Izv. Vyssh. Uchebn. Zaved. Chern. Metall. (1961) 12–20.
53) I. Zaitsev, A. D. Litvina and N. E. Shelkova: High Temp. **39** (2001) 227–232.
54) J. R. A. Carlsson, L. D. Madsen, M. P. Johansson, L. Hultman, X.-H. Li, H. T. G. Hentzell and L. R. Wallenberg: J. Vac. Sci. Tech. A **15** (1997) 8.
55) V. B. Giessen and R. Vogel: Z. Metallkd. **50** (1959) 274–277.
56) J. Korb and K. Hein: Z. Anorg. Allg. Chem. **425** (1976) 281–288.
57) T. Miki, K. Morita and N. Sano: Metall. Mat. Trans. B **27** (1996) 937–941.
58) B. C. Anusionwu, F. O. Ogundare and C. E. Orji: Indian J. Phys. **77A** (2003) 275–279.
59) Y. A. Ugai, L. I. Sokolov, E. G. Goncharov and A. N. Lukin: Izv. Akad. Nauk SSSR, Neorg. Mater. **17** (1981) 1150–1152.
60) K. Uda and M. Kamoshida: J. Appl. Phys. **48** (1977) 18–21.
61) E. Kooi: J. Electrochem. Soc. **111** (1964) 1383–1387.
62) N. K. Abrikosov, V. M. Glazov and L. Chen-Yuan: Rus. J. Inorg. Chem. **7** (1962) 429–431.
63) S. Solmi, A. Parisini, R. Angelucci, A. Armigliato, D. Nobili and L. Moro: Phys. Rev. B **53** (1996) 7836.
64) D. Nobili: 6th. Int. Sympo. Silicon Mater. Technol. Semiconductor, 1990, ed by H. R. Huff, K. Barraclough and J.-I. Chikawa (Electrochem. Soc. 1990), p. 550.
65) M. Tamura: Philos. Mag. **35** (1977) 663–691.
66) K. Yanaba, Y. Matsumura, T. Narushima and Y. Iguchi: Mater. Trans. JIM **39** (1998) 819–823.
67) S. V. Lukin, V. I. Zhuchkov and N. A. Vatolin: J. Less Com. Met. **67** (1979) 399–405.
68) K. Mukai, Z. Yuan, K. Nogi and T. Hibiya: ISIJ Int. **40** (2000) S148–S152.
69) K. Mukai and Z. F. Yuan: Mater. Trans. JIM **41** (2000) 331–337.
70) X. Huang, S. Togawa, S.-I. Chung, K. Terashima and S. Kimura: J. Cryst. Growth **156** (1995) 52–58.
71) Z. Niu, K. Mukai, S. Yutaka, Y. Shiraishi, T. Hibiya, K. Kakimoto and M. Koyama: J. Jpn. Assoc. Cryst. Grow. **23** (1996) 374–381.
72) B. J. Keene: Surf. Inter. Analy. **10** (1987) 367–383.

Appendix: List of Symbols

G_m^{ϕ}: molar Gibbs energy of phase ϕ in a nonmagnetic state
${}^{\mathrm{Ex}}G_m^{\phi}$: excess Gibbs energy of phase ϕ
x_i^{ϕ}: mole fraction of component i in phase ϕ
${}^{k}L_{ij}^{\phi}$: interaction parameter of Redlich-Kister polynomial for i-j binary in phase ϕ
γ_i^{ϕ}: activity coefficient of component i in phase ϕ
$\gamma_i^{i\text{-}j}$: activity coefficient of component i in binary i-j melt
R: universal gas constant
T: absolute temperature
k_i^{eq}: equilibrium distribution coefficient of component i
${}^{V}k_i^{\mathrm{eq}}$: volume equilibrium distribution coefficient of component i
$\Delta^0 G_i^{\mathrm{fus}}$: Gibbs energy of fusion of component i
ΔH_i^m: enthalpy of fusion of component i
ΔS_i^m: entropy of fusion of component i
A: fictitious species, "Area", in the surface phase
A_i: the molar surface areas of pure component i
A_0: the normalization constant
σ_i: surface tension of pure element i
μ_i^0: chemical potential of component i in the bulk phase
μ_i^{S}: chemical potential of component i in the surface phase
a_i^{B}: activity of element i in the bulk phase
a_i^{S}: activity of element i in the surface phase
a_{il}^{B}: coefficients of the stoichiometry matrices of components in bulk phase
a_{il}^{S}: coefficients of the stoichiometry matrices of components in surface phase
n_i^{B}: molar numbers of species in the bulk phase
n_i^{S}: molar numbers of species in the surface phase
b_l: total molar amount of system component l
K_{SiC}^0: equilibrium constant for the reaction $\underline{\mathrm{Si}} + \underline{\mathrm{C}} = \mathrm{SiC}_{\beta}$
${}^{2}k_i^{\mathrm{eq}}$: equilibrium distribution coefficient of i in Si-i binary system
${}^{3}k_i^{\mathrm{eq}}$: equilibrium distribution coefficient of i in Si-i-j ternary system